THE JOURNAL OF PHYSICAL CHEMISTRY A

Article

Cite This: J. Phys. Chem. A 2019, 123, 73−81

pubs.acs.org/JPCA

CO_2/O_2 Exchange in Magnesium−Water Clusters $Mg^+(H_2O)_n$

Erik Barwa, Milan Ončák,* Tobias F. Pascher, Thomas Taxer, Christian van der Linde, and Martin K. Beyer*

Institut für Ionenphysik und Angewandte Physik, Universität Innsbruck, Technikerstraße 25, 6020 Innsbruck, Austria

Supporting Information

ABSTRACT: Hydrated singly charged metal ions doped with carbon dioxide, $Mg^{2+}(CO_2)^-(H_2O)_n$, in the gas phase are valuable model systems for the electrochemical activation of CO_2. Here, we study these systems by Fourier transform ion cyclotron resonance (FT−ICR) mass spectrometry combined with *ab initio* calculations. We show that the exchange reaction of CO_2 with O_2 proceeds fast with bare $Mg^+(CO_2)$, with a rate coefficient $k_{abs} = 1.2 \times 10^{-10}$ cm^3 s^{-1}, while hydrated species exhibit a lower rate in the range of $k_{abs} = (1.2–2.4) \times 10^{-11}$ cm^3 s^{-1} for this strongly exothermic reaction. Water makes the exchange reaction more exothermic but, at the same time, considerably slower. The results are rationalized with a need for proper orientation of the reactants in the hydrated system, with formation of a $Mg^{2+}(CO_4)^-(H_2O)_n$ intermediate while the activation energy is negligible. According to our nanocalorimetric analysis, the exchange reaction of the hydrated ion is exothermic by −1.7 ± 0.5 eV, in agreement with quantum chemical calculations.

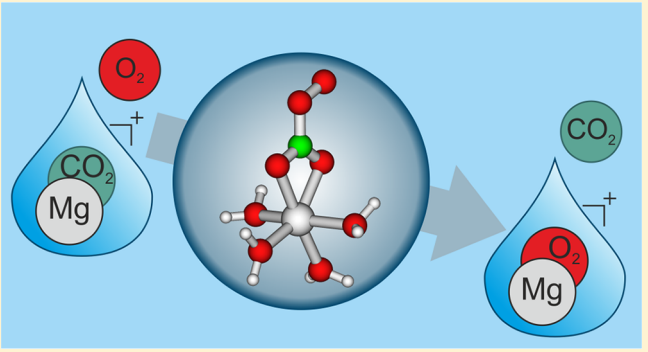

INTRODUCTION

Because of the still increasing consumption of fossil fuels, carbon dioxide is one of the most problematic greenhouse gases produced by humankind. As CO_2 is highly thermodynamically stable, it cannot be easily activated in chemical reactions, and its utilization is very limited.[1] For the transformation of CO_2 to fuels, activation is usually achieved under high temperature and pressure conditions over heterogeneous catalysts in the Sabatier process.[2] A promising alternative is electrochemical activation of CO_2, and the formation of formic acid in electrochemical cells has been reported as early as in 1870.[3] A key intermediate is the carbon dioxide radical anion CO_2^-, which has attracted growing attention in gas phase studies since Compton and Klots reported its stabilization by solvation.[4−6] Carbon dioxide activation in the gas phase was recently reviewed by Weber[7,8] and Schwarz.[9]

Photodissociation of the C−O bond in $CO_2^-(H_2O)_n$ has been reported by Sanov and co-workers.[10,11] In aqueous solution, spectra of CO_2^- in the UV[7,12,13] have been measured, and the symmetric stretching and bending modes have recently been identified by Raman spectroscopy.[14] In gas phase clusters, infrared spectra of $CO_2^-(H_2O)_n$ have been obtained with up to two water molecules in the O−H stretch region.[7,15] Reactions of hydrated electrons with CO_2 directly revealed the process of reductive activation, resulting in the formation of $CO_2^-(H_2O)_n$.[16−21] C−H, C−C, and C−S bond formation was observed with a series of reactants.[22−26] Uggerud and co-workers have shown in elegant studies that $ClMgCO_2^-$ complexes can be formed by collision induced dissociation of the oxalic acid complex, and studied the reactivity of reductively activated CO_2.[27−30] Weber and co-workers investigated reductive CO_2 activation in $M^-(CO_2)_n$ systems by infrared spectroscopy.[7,8,31] Menges et al. demonstrated the capture of CO_2 by a cationic Ni(I) complex and characterized of the activated CO_2 molecule by cryogenic infrared spectroscopy.[32] The Johnson group recently also characterized radical ion adducts between imidazole and CO_2 by vibrational spectroscopy.[33]

In the present work, we are interested in the influence of metal centers on the reactivity of CO_2^- in water clusters, choosing magnesium as a well-investigated metal. Magnesium has also atmospheric relevance as roughly 5 tons of Mg as interplanetary dust enters earth's atmosphere every day.[34] By photoionization or charge transfer reactions with NO^+ and O_2^+, Mg^+ is formed, which further reacts with its surroundings in the mesosphere and lower thermosphere, *inter alia*, with CO_2 and O_2.[35]

Bond dissociation energies for Mg^+ complexes with a series of small molecules, including CO_2, as well as the binding energies of the first four water molecules were determined by collision-induced dissociation (CID) experiments by the Armentrout group.[36,37] Williams and co-workers studied doubly charged hydrated magnesium by blackbody infrared radiative dissociation (BIRD).[38] Singly charged hydrated magnesium ions $Mg^+(H_2O)_n$ have been examined with respect

Received: October 29, 2018
Revised: December 3, 2018
Published: December 5, 2018

DOI: 10.1021/acs.jpca.8b10530
J. Phys. Chem. A 2019, 123, 73−81

to the influence of blackbody infrared radiation, photodissociation, and reactions with small molecules by FT-ICR mass spectrometry and methods of theoretical chemistry.[39−54]

Duncan et al. investigated infrared photodissociation spectroscopy of $Mg^+(CO_2)_n$ and $Mg^+(CO_2)_n$ Ar ion−molecule complexes[55] as well as $Mg^+(H_2O)Ar_n$[56] and Mg^+CO_2.[57] The reactions of hydrated magnesium cations and first-row transition metal ions with CO_2 as well as O_2 were recently explored by van der Linde et al.[54,58] For M = Mg, Cr and Co, charge transfer from metal centers leads to uptake of CO_2 by the positively charged hydrated metal ions, forming $M^{2+}(CO_2)^-(H_2O)_n$ with low efficiency in collisions of $M^+(H_2O)_n$ with CO_2.[54,59] Quantum chemical calculations corroborate that charge transfer occurs, resulting in a doubly charged metal center and a negative $CO_2^{\bullet -}$.[53,54] Similar reactions are observed with O_2 for M = Mg, Cr, Co, Ni, and Zn.

The calculations also show that $Mg^{2+}(CO_2)^-(H_2O)_n$ as well as $Mg^{2+}(O_2)^-(H_2O)_n$ may exist as either solvent-separated ion pairs (SSIP) or contact ion pairs (CIP) whereby the SSIP is the energetically more stable configuration for $n = 16$.[54] Since the electron is located in the valence shell of CO_2 or O_2, the hydrogen loss observed for $Mg^+(H_2O)_n$ clusters, $6 < n < 14$,[60] does not take place. While CO_2 reacts $2-3$ times faster with hydrated electrons than O_2,[61] a different behavior is observed in the case of hydrated Mg^+: O_2 is $4-5$ times more reactive with $[Mg(H_2O)_n]^+$ than CO_2.[54] In the reaction of $CO_2^-(H_2O)_n$ ions with O_2, CO_4^- is very likely formed as an intermediate,[21] as suggested by Weber.[7] Previous theoretical calculations[54] predicted that for clusters with 16 water molecules attached, the reaction energy of the O_2/CO_2 exchange reaction is about −1.86 eV.

To test this prediction experimentally, we investigate the CO_2/O_2 exchange reaction in $Mg^{2+}(CO)_2^-(H_2O)_n$ cluster distributions along with nanocalorimetric analysis[20] of clusters $n \leq 70$. Quantum chemical calculations are used to map possible reaction pathways for both bare and hydrated clusters, respectively, and to monitor the course of the exchange reaction.

EXPERIMENTAL AND THEORETICAL METHODS

The experiments are performed on a modified 4.7 T FT−ICR Bruker/Spectrospin CMS47X mass spectrometer[62] equipped with a Bruker infinity cell[63] and an external laser vaporization source.[64,65] A frequency doubled Nd:YAG laser (Continuum Surelite II) is used to generate $Mg^{2+}(CO_2)^-(H_2O)_n$ ions by evaporation of isotopically enriched ^{24}Mg from a solid metal target and supersonic jet expansion of a hot plasma in a helium/water/CO_2 gas mixture. Twenty laser shots at 10 Hz and approximately 5 mJ pulse energy are used to generate the ions. The ions are rotationally and vibrationally cooled below room temperature due to the supersonic expansion into high vacuum, accelerated downstream from a skimmer and transferred to the ICR cell by a system of electrostatic lenses through several differential pumping stages.[66] In the ICR cell, ions are stored at room temperature in an electromagnetic trap under ultrahigh vacuum conditions in a 4.7 T magnetic field.[67] O_2 is introduced at constant backing pressure, allowing the monitoring of reaction kinetics by taking mass spectra after different reaction delays. For each mass spectrum, 20 experiment cycles are averaged.

Absolute rate coefficients k_{abs} are obtained by analyzing the pseudo-first-order kinetic plots of different experimental runs taken over a range of pressures. The cluster distribution shrinks due to blackbody infrared radiative dissociation (BIRD)[68−76] and the exothermicity of the reaction.[58,77,78] The error of the rate coefficient was estimated to be about 30% due to the uncertainty of the pressure calibration.[79,80] The noise level of the summed intensities was calculated with the Gaussian law of error propagation from the noise level of each peak. It should be noted that the internal temperature of the clusters is given by the interplay between radiative heating and evaporative cooling. Experiments on phase transitions in water clusters place this temperature in the region of 100−200 K.[81,82]

The collision rates k_{ADO}, k_{HSA} and k_{SCC} are calculated using the average dipole orientation (ADO),[83,84] hard sphere average dipole orientation (HSA) and surface charge capture (SCC) models, which yield the efficiencies $\Phi_{ADO} = k_{abs}/k_{ADO}$, $\Phi_{HSA} = k_{abs}/k_{HSA}$, and $\Phi_{SCC} = k_{abs}/k_{SCC}$, respectively.[85] Nanocalorimetric analysis is performed by fitting the average cluster size $\langle n \rangle$ of reactant and product ions over time with a set of differential equations, which yields the average number of water molecules evaporating due to the heat of the reaction.[20,21,61] The evaporation of one H_2O molecule removes $\Delta E_{vap} = 0.45 \pm 0.03$ eV from the cluster.[82,86]

Selected clusters were optimized using the M06 density functional theory (DFT) functional[87] along with the def2TZVP basis set. As the DFT theory might struggle to quantitatively describe the nature of the Mg^+/O_2 interaction,[88] we recalculated the structures using the complete basis set QB3 (CBS-QB3) method.[89] This method is able to reproduce values calculated at the coupled cluster level (CCSD(T)/aug-cc-pVQZ) as already noted elsewhere.[88] Molecular volume calculations for the HSA and SCC methods and charge analysis within the ChelpG scheme[90] were performed at the MP2/def2TZVP level.

Molecular dynamics was run on the M06/6-31+G* potential energy surface with a time step of 30 au (~0.75 fs). Investigated $[Mg(CO_2)(H_2O)_n]^+$ clusters were first thermalized at 250 K using the Nosé−Hoover thermostat. Then, an O_2 molecule was added at a distance of 10 Å with respect to the cluster center of mass and a microcanonical simulation was performed. Twenty trajectories were run for each structure. A dynamics run was stopped when a neutral molecule (O_2 or CO_2) leaves the cluster by more than 10 Å or after 7 ps (or 12 ps when CO_4^- was formed to investigate its dissociation). We considered only runs, either reactive or nonreactive, where O_2 approached the cluster with a distance shorter than 3 Å with respect to any cluster atom.

All quantum chemical calculations were performed in the Gaussian program,[91] the Abin code was used for molecular dynamics.[92] For calculation of unimolecular rate constants, a standard RRKM implementation was used.[93]

RESULTS AND DISCUSSION

We investigate the O_2/CO_2 exchange reaction in the $Mg^{2+}(CO_2)^-(H_2O)_n$ ion:

$$Mg^{2+}(CO_2)^-(H_2O)_n + O_2 \rightarrow Mg^{2+}(O_2)^-(H_2O)_{n-m} + CO_2 + mH_2O \quad (1)$$

Measured rate coefficients of reaction 1 for various average cluster sizes are collected in Table 1, calculated reaction energies for $n = 0-7$ are shown in Table 2.

DOI: 10.1021/acs.jpca.8b10530
J. Phys. Chem. A 2019, 123, 73−81

Table 1. Measured Rate Coefficients k_{abs} and Efficiencies Φ_{HSA}, Φ_{SCC}, and Φ_{ADO} for O_2/CO_2 Exchange Reaction 1 with Different Average Cluster Size n of the Initial $Mg^{2+}(CO_2)^-(H_2O)_n$ Cluster and Their Associated Mean Energy Release ΔE_{nc} Calculated from the Evaporated Number of Water Molecules ΔN_{vap}

n	k_{abs} [10^{-11} cm^3 s^{-1}]	Φ_{HSA} [%]	Φ_{SCC} [%]	Φ_{ADO} [%]	ΔN_{vap}	ΔE_{nc} [eV]
0	12.3	–	–	21	–	–
7	2.2	3.0	1.6	–	–	–
20	1.2	1.6	0.7	–	–	–
36	1.6	1.7	0.8	–	4.3	1.9
43	1.9	1.9	0.9	–	3.1	1.4
55	2.4	1.9	0.9	–	3.6	1.6

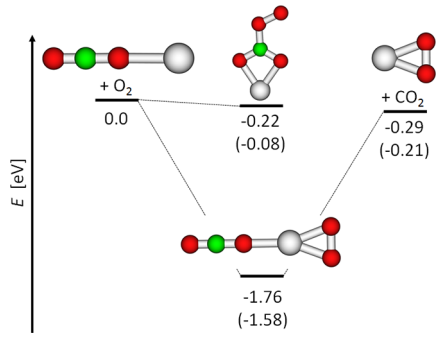

Figure 1. Calculated reaction profile for reaction of $[MgCO_2]^+$ with O_2. Calculated energies (in eV) are given at the CBS-QB3 and M06/def2TZVP (in parentheses) levels of theory.

The Nonhydrated Species $Mg^+(CO_2)$. First, we discuss the O_2/CO_2 reaction for $n = 0$, i.e., the conversion from $Mg^+(CO_2)$ to $Mg^{2+}(O_2)^-$. This reaction proceeds with a relatively high rate coefficient of $k_{abs} = 1.2 \times 10^{-10}$ cm^3 s^{-1} resulting in an efficiency of $\Phi_{ADO} = 21\%$. The same reaction was previously examined in a fast flow tube-mass spectrometer at a pressure of 1.2 Torr, with a measured rate coefficient roughly five times smaller than in our experiment,[35,94] probably due to the different pressure. In the fast flow tube-mass spectrometer experiment, the $[(CO_2)Mg(O_2)]^+$ complex was also observed, which got stabilized in collisions with background gas.[35] Since the pressure in our chamber is 7 orders of magnitude lower than in the fast flow tube, there are nearly no collisions, resulting in immediate elimination of the CO_2 molecule.

The calculated exchange reaction energy is −0.29 eV (at the CBS-QB3 level), the respective reaction profile is shown in Figure 1. Theoretical calculations predict that $Mg^+(CO_2)$ is linear while $Mg^{2+}(O_2)^-$ has C_{2v} symmetry, as pointed out before.[88] Analysis of atomic charges shows that these two ions have considerably different electronic structures: The bonding in $Mg^+(CO_2)$ can be best described as an ion-induced dipole interaction, with a charge transfer of −0.29 e from CO_2 to Mg^+ ($q_{Mg} = 0.71$ e), because the linear CO_2 is reluctant to accept an electron. In $Mg^{2+}(O_2)^-$, a considerable charge transfer from Mg^+ to O_2 is observed ($q_{Mg} = 1.63$ e).

The O_2/CO_2 exchange reaction on Mg^+ is predicted to follow a direct pathway, with adsorption of O_2 followed by dissociation of CO_2. The energy released during the formation of the $[(CO_2)Mg(O_2)]^+$ encounter complex (~1.8 eV) easily induces dissociation of the CO_2 unit in the absence of stabilizing collisions. In the $[(CO_2)Mg(O_2)]^+$ structure, there is already a considerable charge transfer from Mg ($q_{Mg} = 1.34$ e) toward O_2 ($q_{O_2} = -0.55$ e). The high stability of $[CO_2MgO_2]^+$ is in agreement with its observation in the above-mentioned flow tube experiment.[35]

The $Mg^{2+}(CO_4)^-$ structure is a local minimum on the potential energy surface, with the charge on Mg calculated as $q_{Mg} = 1.68$ e. However, its formation requires considerable cluster reorganization, and it is stabilized by only ~0.2 eV (Figure 1) relative to $Mg^+(CO_2)$. For energetic as well as mechanistic reasons, we do not expect an $Mg^{2+}(CO_4)^-$ intermediate to be formed in our experiment.

The course of the $Mg^+(CO_2) + O_2$ reaction was further studied by molecular dynamics (see Table 3 and the SI). Only two channels were observed during the simulation time (7 ps), viz. formation of $[(CO_2)Mg(O_2)]^+$ (75%) and scattering of O_2 on the $Mg^+(CO_2)$ ion when O_2 approaches the ion from the side of the CO_2 (25%). We observed no elimination of CO_2 on the time scale of 7 ps. This can be understood considering the high dissociation energy of CO_2 from $Mg^{2+}(O_2)^-$ (Figure 1). According to our RRKM calculations, the rate of CO_2 dissociation is about 5×10^5 s^{-1} when disregarding thermal energy of the cluster, using energetics and frequencies calculated at the M06/def2TZVP level. Thus, on the time scale of the experiment (i.e., seconds), energy redistribution takes place and CO_2 dissociates.

The Hydrated Species $Mg^{2+}(CO_2)^-(H_2O)_n$. When the $Mg^+(CO_2)$ core is hydrated to $Mg^{2+}(CO_2)^-(H_2O)_n$, different reactivity patterns are observed. Figure 2 shows the mass spectra at an O_2 pressure of 6.4×10^{-8} mbar after different delays. The corresponding reaction kinetics can be seen in Figure 3a. After 4 s, more than half of $Mg^{2+}(CO_2)^-(H_2O)_n$ ions were converted to $Mg^{2+}(O_2)^-(H_2O)_n$. No reaction with a second oxygen molecule was observed. At the same time, the $[(CO_2)Mg(O_2)(H_2O)_n]^+$ complex was not observed, suggesting that CO_2 leaves the cluster soon after O_2 uptake. The absence of $[(CO_2)Mg(O_2)(H_2O)_n]^+$ in the FT-ICR mass spectra places an upper limit of ~100 ms on the lifetime of these species, but it can be expected that the actual lifetime is significantly shorter.

Table 2. Reaction Energies (in eV) of Hydration of $Mg^{2+}(CO_2)^-(H_2O)_n$ and $Mg^{2+}(O_2)^-(H_2O)_n$ Clusters, the CO_2/O_2 Exchange Reaction, and CO_4 Formation, Calculated at the CBS-Q3 Level of Theory

reaction	n = 0	1	2	3	4	5	6	7
$Mg^{2+}(CO_2)^-(H_2O)_n + H_2O \rightarrow Mg^{2+}(CO_2)^-(H_2O)_{n+1}$	−1.14	−1.19	−1.31	−0.90	−0.77	−0.68	−0.58	-
$Mg^{2+}(O_2)^-(H_2O)_n + H_2O \rightarrow Mg^{2+}(O_2)^-(H_2O)_{n+1}$	−2.19	−1.67	−1.30	−0.92	−0.63	−0.59	−0.63	-
$Mg^{2+}(CO_2)^-(H_2O)_n + O_2 \rightarrow Mg^{2+}(O_2)^-(H_2O)_n + CO_2$	−0.29	−1.34	−1.82	−1.80	−1.82	−1.69	−1.60	−1.64
$Mg^{2+}(CO_2)^-(H_2O)_n + O_2 \rightarrow Mg^{2+}(CO_4)^-(H_2O)_n$	−0.22	−1.20	−1.66	−1.67	−1.66	−1.63	−1.64	−1.68

DOI: 10.1021/acs.jpca.8b10530
J. Phys. Chem. A 2019, 123, 73−81

Table 3. Reaction Channels (in %) Observed during Molecular Dynamics for Four Selected $Mg^{2+}(CO_2)^-(H_2O)_n$ Clusters[a]

reaction channel	$Mg^+(CO_2)$	$Mg^{2+}(CO_2^-)(H_2O)_2$	$Mg^{2+}(CO_2)^-(H_2O)_5$, **Va**	$Mg^{2+}(CO_2)^-(H_2O)_5$, **Vb**
scattering, i.e., $[Mg(CO_2)(H_2O)_n]^+ + O_2$	25	60	70	85
$Mg^{2+}(O_2)^-(H_2O)_n + CO_2$	0	35	10	0
$[(CO_2)Mg(O_2)(H_2O)_n]^+$	75	0	5	0
$Mg^{2+}(CO_4)^-(H_2O)_n$	0	5	15	15

[a]A total of 20 molecular dynamics runs on the M06/6-31+G* potential energy surface were performed for each isomer, with total time of 7 ps (prolonged to 12 ps when the CO_4 moiety is formed). The O_2/CO_2 exchange reaction proceeds either directly on the Mg^+ core (for $Mg^{2+}(CO_2)^-(H_2O)_2$) or through CO_4^- formation (for $Mg^{2+}(CO_2)^-(H_2O)_5$).

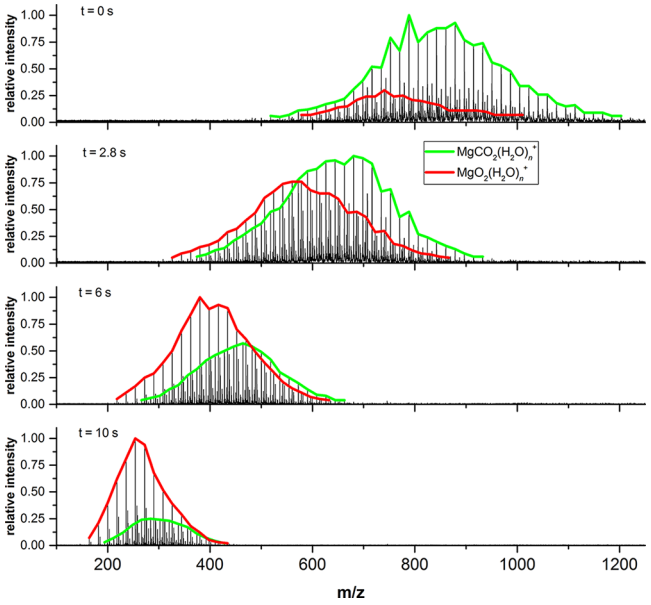

Figure 2. Mass spectra of the reaction of $[Mg(CO_2)(H_2O)_n]^+$ with O_2 at a pressure of 6.4×10^{-8} mbar after 0, 2.8, 6 and 10 s. Quantitative formation of $Mg(O_2)(H_2O)_{n-x}^+$ was observed.

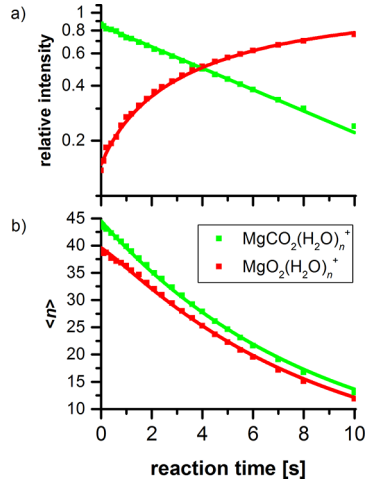

Figure 3. (a) Reaction kinetics of reaction 1 extracted from the mass spectra seen in Figure 2. (b) Average cluster size $\langle n \rangle$ of $[Mg(CO_2)(H_2O)_n]^+$ and $[Mg(O_2)(H_2O)_n]^+$. Clusters shrink due to the exothermicity of the reaction and BIRD.

Figure 3b summarizes the average cluster size $\langle n \rangle$ of reactant and product as a function of time. A nanocalorimetric fit yields the number of water molecules that evaporate due to the reaction. In the first 10 s, BIRD has a large influence on the average cluster size. The BIRD rate decreases with decreasing size.[70,74] When $n = 3$ is reached, no further dissociation is observed on the time scale of the experiment.

A mean rate coefficient $k_{abs} = 1.5 \times 10^{-11}$ cm^3 s^{-1} has been obtained for $n \geq 20$, with similar rate coefficients in the n = 20−55 range (see Table 1). For a cluster with 43 water molecules, reaction efficiency is predicted to be $\Phi_{HSA} = 1.9\%$ and $\Phi_{SCC} = 0.9\%$. The actual efficiency might lie somewhere in between, i.e. about one in 70 collisions is reactive. Compared to the complex without water molecules, the exchange reaction is an order of magnitude slower.

For the quantitative nanocalorimetric analysis, only data were fitted with a starting average cluster size of $n \geq 36$ to minimize the influence of the size dependent rate coefficient. The mean energy release of reaction 1 corresponds to $\Delta E_{nc}(1) = 1.7 \pm 0.5$ eV, and the mean number of evaporated water molecules $m = 3.8$ as calculated for clusters with $n \geq 36$ and averaged over six measurements. The energy is, within the experimental uncertainty, identical to the value of $\Delta E_{nc}(2) = 1.5 \pm 0.3$ eV measured in a previous study for the reaction without the magnesium core, reaction 2.[21]

$$(CO_2)^-(H_2O)_n + O_2 \rightarrow (O_2)^-(H_2O)_{n-m} + CO_2 + mH_2O \quad (2)$$

To understand the reaction mechanism, in particular whether formation of a $Mg^{2+}(CO_4)^-(H_2O)_n$ intermediate is required, we calculated structures of $Mg^{2+}(CO_2)^-(H_2O)_n$, $Mg^{2+}(O_2)^-(H_2O)_n$ and $Mg^{2+}(CO_4)^-(H_2O)_n$ clusters for n = 1−7 as shown in Figure 4. The calculated energies of hydration and exchange reactions are collected in Table 2. When Mg^+CO_2 is hydrated by one water molecule, there are two possible isomers with different electronic structure. The more stable isomer **Ia** with linear CO_2 shows a very limited charge transfer, and electron density is actually transferred from CO_2 to $Mg^+(H_2O)$ ($q_{CO_2} = 0.29$ e). In isomer **Ib**, which lies 0.44 eV above **Ia**, CO_2 is coordinated in bidentate fashion to Mg^+, and a considerable charge transfer to CO_2 takes place ($q_{CO_2} = -0.63$ e).

For two water molecules, CO_2 connected to Mg^+ already tends to accept an electron, loses its linearity, and binds either in monodentate or bidentate fashion. The structure with linear CO_2 (**IIb**) is also local minimum on the potential energy surface, but is higher in energy. The bidentate motif is predicted to be the most stable one for $n = 1-4$. However, there is only a small energy difference between monodentate and bidentate structures. Already, for $n = 7$, the bidentate structure collapses during optimization into a monodentate structure. For $n = 6-7$, we also optimized two structures where CO_2 is not directly attached to Mg^+ (**VId**, **VIIb**). However, this configuration is less stable by about 0.7 eV.

For all structures with at least 2 water molecules, the charge transfer from Mg^+ to CO_2 is already substantial, with the CO_2

DOI: 10.1021/acs.jpca.8b10530
J. Phys. Chem. A 2019, 123, 73−81

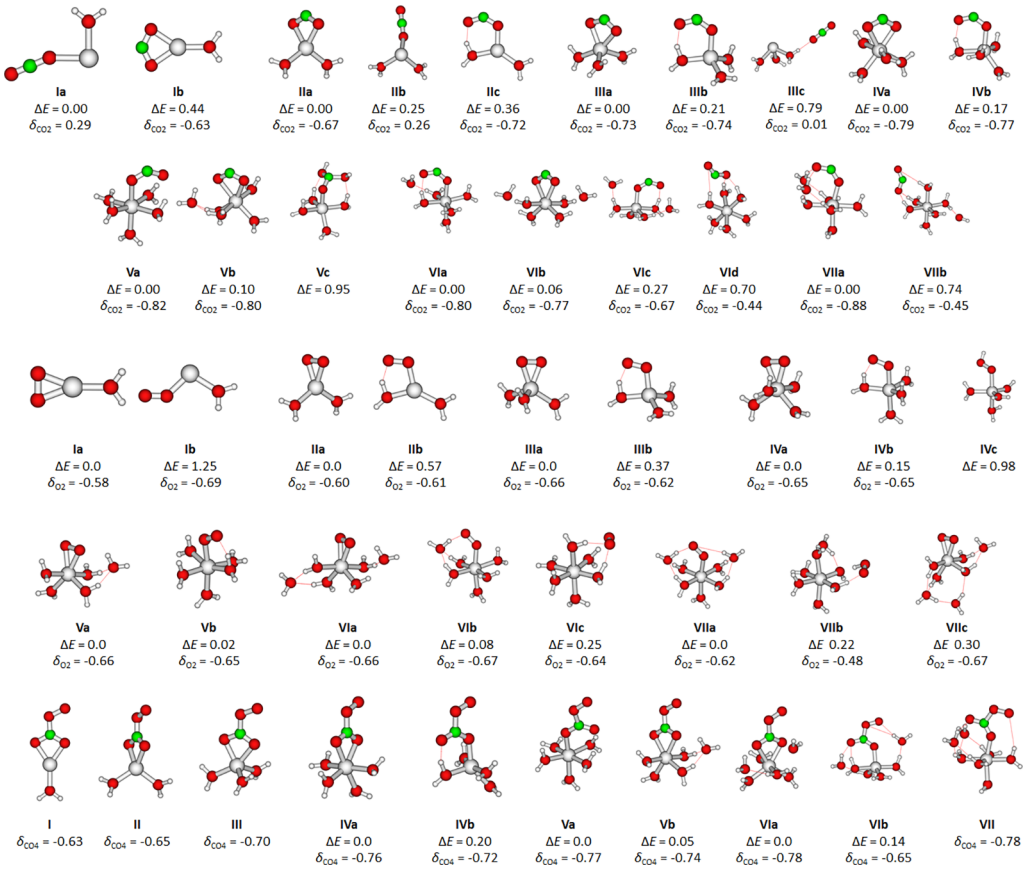

Figure 4. Calculated structures of selected $[Mg(CO_2)(H_2O)_n]^+$, $[Mg(O_2)(H_2O)_n]^+$ and $[Mg(CO_4)(H_2O)_n]^+$ clusters along with relative energy (in eV) and charge on the CO_2 or O_2 unit (in e), at the CBS-QB3 level of theory. Charges were retrieved using the CHELPG scheme at the MP2/def2TZVP level of theory.

charge of about (−0.9 − −0.6) e for both monodentate and bidentate structure. The structure of hydrated $Mg^+(CO_2)$ clusters can be thus described as $Mg^{2+}(CO_2)^-(H_2O)_n$. Even in the structure with CO_2 not directly attached to Mg^+ (**VId**, **VIIb**), about −0.5 e is transferred to CO_2. This inefficient charge transfer can also explain the relative instability of this structure.

For O_2 attached to hydrated Mg^+, bidentate binding seems to be more favorable, but the difference relative to the monodentate structure is negligible for $n > 3$. For $n = 6–7$, structures without direct O_2−Mg^+ interaction were also considered (**VIc**, **VIIb**). These structures are only about 0.25 eV less stable with respect to structures with Mg^+-coordinated O_2. At the same time, an HO_2 radical might be formed (**VIIb**), with the proton transfer favored by the strongly polarizing Mg^{2+} center.

The calculated energies released in the O_2/CO_2 exchange reaction 1 amount to about (−1.8 − −1.6) eV for $n \geq 2$, while n = 0, 1 feature lower exothermicity (see Table 2). In other words, the reaction energy seems to converge already for $n = 2$, with only limited changes with ongoing hydration, irrespective whether a water molecule is added in the first or second solvation shell. This can be traced to similar hydration energies for clusters with CO_2 and O_2. The calculated reaction energy agrees within error limits with the experimentally measured value.

In a previous publication,[21] a prominent role of the CO_4^- ion was suggested for reaction 2, as previously predicted by Weber.[7] CO_4^- formation on a hydrated $Mg^{2+}(CO_2)^-$ center is also strongly exothermic, with a release of 1.6−1.7 eV for $n > 1$.

For both O_2/CO_2 exchange reaction and CO_4^- formation on $Mg^{2+}(CO_2)^-(H_2O)_n$, reaction exothermicity increases considerably for $n > 1$. However, the exchange reaction on a hydrated cluster is found to proceed much slower in the experiment, compared to reactivity of bare $Mg^+(CO_2)$. This effect must be caused by water molecules already in the first hydration layer, as a small rate coefficient is observed even for $n = 7$ where the second hydration layer does not contain more than three water molecules. To determine the reaction mechanism and the role of the Mg^+ ion in the process, we investigated the exchange reaction using both time-independent calculations and molecular dynamics simulations.

In Figure 5, we analyze reaction mechanisms through relaxed scans along the potential energy surface. Three reaction mechanisms were considered. For two reactions proceeding through direct charge transfer (a, b), we follow the CO_2 angle as the reaction coordinate. For CO_2^-, an angle of about 135° is expected, neutral CO_2 is linear. In $Mg^{2+}(CO_2)^-(H_2O)_5$ **Va** (Figure 5a), the reaction is hindered by the reorganization of the hydrogen bonded network, with a barrier below 0.2 eV. When the CO_2 molecule starts to linearize, its charge diminishes, it is pushed out of the cluster and an HO_2 moiety is formed. For $Mg^{2+}(CO_2)^-(H_2O)_6$ with CO_2 in the second solvation shell (Figure 5b), the reaction barrier further decreases and could not be determined unequivocally. Again, the charge transfer leads to linearization of CO_2 and formation of an HO_2 moiety.

DOI: 10.1021/acs.jpca.8b10530
J. Phys. Chem. A 2019, 123, 73−81

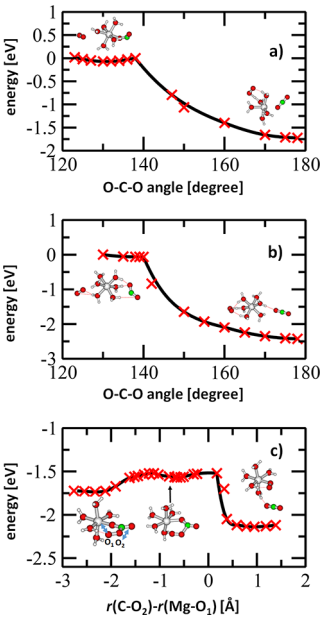

Figure 5. Possible reaction mechanisms for the O_2/CO_2 exchange calculated as relaxed scans along selected reaction coordinates (CO_2 angle or CO_4^- decomposition) at the M06/def2TZVP level of theory, energy is shown with respect to the entrance channel of the respective structure, i.e., $Mg^{2+}(CO_2)^-(H_2O)_n + O_2$. (a) Direct O_2/CO_2 exchange reaction on the Mg^+ center. (b) O_2/CO_2 exchange reaction remote from the Mg^+ center. (c) Formation of $Mg^{2+}(O_2)^-$ core through CO_4^- ion decomposition.

The third reaction scenario proceeds through formation of CO_4^- and direct CO_2/O_2 exchange on the Mg^+ center (Figure 5c). The pathway does not require a high activation energy (~0.1 eV) and lies well under the entrance channel energy; however, a suitable initial structure with a low O_2...Mg distance has to be reached. We also considered oxygen atom exchange between O_2 and CO_2 on the Mg center, the respective barrier was however found to exceed the entrance channel energy and we do not expect this process to take place.

To understand the role of hydration and the difference between reactivity of singly and doubly coordinated CO_2, we study reactivity of $Mg^{2+}(CO_2)^-(H_2O)_n$ clusters toward O_2 using molecular dynamics. Three structures were selected, **IIa**, **Va**, and **Vb**. Because of the expected low efficiency of the reaction, we performed the dynamics at 250 K, i.e. at higher temperature than the internal temperature of the clusters of about 100−200 K. The results are collected in Table 3, selected videos of MD runs are provided in the Supporting Information.

When we compare reaction channels observed for $Mg^+(CO_2)$ and $Mg^{2+}(CO_2)^-(H_2O)_2$, a strong influence of hydration can be observed. First, the ratio of scattering reactions increases about twice due to water molecules hindering the approach to the Mg^+ core. Second, complexation observed for $Mg^+(CO_2)$ is here substituted by the exchange reaction that is seen in 35% of cases (note the high reaction energy of about −1.8 eV in Table 2). In one case, formation of a long-living CO_4^- was observed.

For isomers **Va** and **Vb**, we saw similar reaction channels. Scattering of O_2 from the ion is the most important channel (70% and 85%, respectively), followed by CO_4^- formation (15% for both isomers). For isomer **Va**, dissociation of CO_4^- to form a $Mg^{2+}(O_2)^-$ core is observed in two dynamic runs, following the reaction pathway suggested in Figure 5c. Finally, a $Mg^+(CO_2)$ core with a loosely attached O_2 was also observed for **Va** (5%).

Ligand exchange through CO_4^- formation is the only reaction channel observed for isomers **Va** and **Vb** to produce a $Mg^{2+}(O_2)^-(H_2O)_5$ cluster. Because of the hydration of the Mg^+ core, no direct O_2/CO_2 exchange reaction without CO_4^- formation is documented. The charge exchange suggested in Figure 5a was not seen, probably due to the short time of the respective nonreactive collision. Molecular dynamics results also explain why the exchange reaction proceeds much slower, although the reaction exothermicity increases considerably. After hydration of $Mg^+(CO_2)$, the O_2 molecule must approach the cluster from a suitable direction to form CO_4^-. In calculations, we observe an increase in scattering probability by a factor of ~3 when passing from a bare $Mg^+(CO_2)$ ion to $Mg^+(CO_2)(H_2O)_n$ with $n = 5$, compared to a factor of ~5 in the experiment when comparing $n = 0$ and $n \sim 7$.

Another indication of the increased importance of proper orientation of the impacting O_2 molecule are the results for $CO_2^-(H_2O)_n$. The metal-free species exhibit a 2−3 times higher rate constant for CO_2/O_2 exchange[21] than $Mg^{2+}(CO_2)^-(H_2O)_n$. Without the Mg^+ core, we might expect CO_2^- located on the cluster surface up to larger cluster sizes, thus increasing the reaction cross section. The nanocalorimetric analysis on the $CO_2^-(H_2O)_n$ clusters leads to $\Delta E_{nc} = 1.5 \pm 0.3$ eV,[21] which is slightly lower compared to the present experiment on the Mg^+ core. This supports the assumption that CO_2^- is located on the surface of the $CO_2^-(H_2O)_n$ cluster and bound to a low number of water molecules, resulting in a lower evaporation energy. The measured efficiency is also 50% higher for $CO_2^-(H_2O)_n$ than for $Mg^{2+}(CO_2)^-(H_2O)_n$. The presence of Mg^+ makes the exchange reaction less effective due to the solvation of the $Mg^{2+}(CO_2)^-$ core in the clusters.

CONCLUSION

We studied singly charged hydrated magnesium cations with carbon dioxide, $Mg^{2+}(CO_2)^-(H_2O)_n$, in reaction with neutral molecular oxygen. The reaction is efficient, resulting in an exchange reaction of CO_2 to O_2. For $n = 0$, an absolute rate coefficient $k_{abs} = 1.2 \times 10^{-10}$ cm^3 s^{-1} is measured. For hydrated clusters, the reaction is slower, and we obtained an average of $k_{abs} = 1.5 \times 10^{-11}$ cm^3 s^{-1} for hydration by 20−55 water molecules. This behavior can be rationalized by two different reaction scenarios. For $n = 0$, direct CO_2/O_2 exchange on the Mg^+ core is observed. With hydration, CO_4^- formation seems to be necessary for the reaction to proceed, as indicated by molecular dynamics simulations. Although CO_4^- formation and subsequent dissociation to O_2^- and CO_2 on the hydrated Mg^+ core are considerably more exothermic compared to the reaction on a bare Mg^+ ion, hydration at the same time lowers the reaction cross section for CO_4^- formation on the cluster. This is also indirectly supported by a higher reaction constant observed for the same reaction without the Mg^+ core.[21] For the hydrated clusters, we determined the reaction enthalpy by a nanocalorimetric analysis to be 1.7 ± 0.5 eV, in agreement with the calculated value.

ASSOCIATED CONTENT

Supporting Information

The Supporting Information is available free of charge on the ACS Publications website at DOI: 10.1021/acs.jpca.8b10530.

DOI: 10.1021/acs.jpca.8b10530
J. Phys. Chem. A 2019, 123, 73−81

Cartesian coordinates of all optimized structures (PDF)
Videos from molecular dynamics simulations (ZIP)

AUTHOR INFORMATION

Corresponding Authors

*(M.O.) E-mail: milan.oncak@uibk.ac.at.
*(M.K.B.) E-mail: martin.beyer@uibk.ac.at.

ORCID

Milan Ončák: 0000-0002-4801-3068
Martin K. Beyer: 0000-0001-9373-9266

Notes

The authors declare no competing financial interest.

ACKNOWLEDGMENTS

Financial support from the Austrian Science Fund (FWF), Project No. P 28896, is gratefully acknowledged. M.O. acknowledges support through the Lise Meitner Programme of the FWF, Project No. M2001-NBL. The computational results presented have been achieved using the HPC infrastructure LEO of the University of Innsbruck.

REFERENCES

(1) van Eldik, R.; Aresta, M. *CO_2 Chemistry*; Elsevier Science: 2013.
(2) Centi, G.; Perathoner, S. Opportunities and Prospects in the Chemical Recycling of Carbon Dioxide to Fuels. *Catal. Today* **2009**, *148*, 191−205.
(3) Royer, M. E. Réduction de l'Acide Carbonique en Acide Formique. *Comptes Rendus Acad. Sci.* **1870**, *70*, 731−732.
(4) Klots, C. E.; Compton, R. N. Electron Attachment to Carbon Dioxide Clusters in a Supersonic Beam. *J. Chem. Phys.* **1977**, *67*, 1779−1780.
(5) Klots, C. E. Stable Gas-Phase Hydrates of the CO_2^- Anion. *J. Chem. Phys.* **1979**, *71*, 4172.
(6) Klots, C. E.; Compton, R. N. Electron Attachment to van der Waals Polymers of Carbon Dioxide and Nitrous Oxide. *J. Chem. Phys.* **1978**, *69*, 1636−1643.
(7) Weber, J. M. The Interaction of Negative Charge with Carbon Dioxide − Insight into Solvation, Speciation and Reductive Activation from Cluster Studies. *Int. Rev. Phys. Chem.* **2014**, *33*, 489−519.
(8) Dodson, L. G.; Thompson, M. C.; Weber, J. M. Characterization of Intermediate Oxidation States in CO_2 Activation. *Annu. Rev. Phys. Chem.* **2018**, *69*, 231−252.
(9) Schwarz, H. Metal-Mediated Activation of Carbon Dioxide in the Gas Phase: Mechanistic Insight Derived from a Combined Experimental/Computational Approach. *Coord. Chem. Rev.* **2017**, *334*, 112−123.
(10) Habteyes, T.; Velarde, L.; Sanov, A. Solvent-Enabled Photodissociation of CO_2^- in Water Clusters. *Chem. Phys. Lett.* **2006**, *424*, 268−272.
(11) Habteyes, T.; Velarde, L.; Sanov, A. Photodissociation of CO_2^- in Water Clusters via Renner-Teller and Conical Interactions. *J. Chem. Phys.* **2007**, *126*, 154301.
(12) Neta, P.; Simic, M.; Hayon, E. Pulse Radiolysis of Aliphatic Acids in Aqueous Solutions. I. Simple Monocarboxylic Acids. *J. Phys. Chem.* **1969**, *73*, 4207−4213.
(13) Lin, M.; Katsumura, Y.; Muroya, Y.; He, H.; Miyazaki, T.; Hiroishi, D. Pulse Radiolysis of Sodium Formate Aqueous Solution up to 400°C: Absorption Spectra, Kinetics and Yield of Carboxyl Radical CO_2^-. *Radiat. Phys. Chem.* **2008**, *77*, 1208−1212.
(14) Janik, I.; Tripathi, G. N. R. The Nature of the CO_2^- Radical Anion in Water. *J. Chem. Phys.* **2016**, *144*, 154307.
(15) Muraoka, A.; Inokuchi, Y.; Nishi, N.; Nagata, T. Structures of $[(CO_2)_n(H_2O)_m]^-$ (n = 1−4, m = 1,2) Cluster Anions. I. Infrared Photodissociation Spectroscopy. *J. Chem. Phys.* **2005**, *122*, 094303.
(16) Yang, X.; Castleman, A. W. Chemistry of Large Hydrated Anion Clusters $X(H_2O)_n$, $0 \leq n \approx 50$ and X = OH, O, O_2, and O_3. 1. Reaction of CO_2 and Possible Application in Understanding of Enzymatic Reaction Dynamics. *J. Am. Chem. Soc.* **1991**, *113*, 6766−6771.
(17) Arnold, S. T.; Morris, R. A.; Viggiano, A. A.; Johnson, M. A. Thermal Energy Reactions of Size-Selected Hydrated Electron Clusters $(H_2O)_n^-$. *J. Phys. Chem.* **1996**, *100*, 2900−2906.
(18) Balaj, O. P.; Siu, C. K.; Balteanu, L.; Beyer, M. K.; Bondybey, V. E. Free Electrons, the Simplest Radicals of Them All: Chemistry of Aqueous Electrons as Studied by Mass Spectrometry. *Int. J. Mass Spectrom.* **2004**, *238*, 65−74.
(19) Balaj, O. P.; Siu, C. K.; Balteanu, I.; Beyer, M. K.; Bondybey, V. E. Reactions of Hydrated Electrons $(H_2O)_n^-$ with Carbon Dioxide and Molecular Oxygen: Hydration of the CO_2^- and O_2^- Ions. *Chem. - Eur. J.* **2004**, *10*, 4822−4830.
(20) Höckendorf, R. F.; Balaj, O. P.; van der Linde, C.; Beyer, M. K. Thermochemistry from Ion−Molecule Reactions of Hydrated Ions in the Gas Phase: A New Variant of Nanocalorimetry Reveals Product Energy Partitioning. *Phys. Chem. Chem. Phys.* **2010**, *12*, 3772−3779.
(21) Akhgarnusch, A.; Tang, W. K.; Zhang, H.; Siu, C.-K.; Beyer, M. K. Charge Transfer Reactions between Gas-Phase Hydrated Electrons, Molecular Oxygen and Carbon Dioxide at Temperatures of 80−300 K. *Phys. Chem. Chem. Phys.* **2016**, *18*, 23528−23537.
(22) Höckendorf, R. F.; Siu, C.-K.; van der Linde, C.; Balaj, O. P.; Beyer, M. K. Selective Formic Acid Synthesis from Nanoscale Electrochemistry. *Angew. Chem., Int. Ed.* **2010**, *49*, 8257−8259.
(23) Höckendorf, R. F.; Hao, Q.; Sun, Z.; Fox-Beyer, B. S.; Cao, Y.; Balaj, O. P.; Bondybey, V. E.; Siu, C.-K.; Beyer, M. K. Reactions of CH_3SH and CH_3SSCH_3 with Gas-Phase Hydrated Radical Anions $(H_2O)_n^{\bullet-}$, $CO_2^{\bullet-}(H_2O)_n$, and $O_2^{\bullet-}(H_2O)_n$. *J. Phys. Chem. A* **2012**, *116*, 3824−3835.
(24) Höckendorf, R. F.; Fischmann, K.; Hao, Q.; van der Linde, C.; Balaj, O. P.; Siu, C.-K.; Beyer, M. K. C−C Bond Formation between $CO_2^{\bullet-}$ and Allyl Alcohol: A Mechanistic Study. *Int. J. Mass Spectrom.* **2013**, *354*−*355*, 175−180.
(25) Akhgarnusch, A.; Höckendorf, R. F.; Hao, Q.; Jäger, K. P.; Siu, C.-K.; Beyer, M. K. Carboxylation of Methyl Acrylate by Carbon Dioxide Radical Anions in Gas-Phase Water Clusters. *Angew. Chem., Int. Ed.* **2013**, *52*, 9327−9330.
(26) Herburger, A.; Ončák, M.; Barwa, E.; van der Linde, C.; Beyer, M. K. Carbon-Carbon Bond Formation in the Reaction of Hydrated Carbon Dioxide Radical Anions with 3-Butyn-1-ol. *Int. J. Mass Spectrom.* **2019**, *435*, 101−106.
(27) Dossmann Soldi-Lose, H.; Afonso, C.; Lesage, D.; Tabet, J.-C.; Uggerud, E. Formation and Characterization of Gaseous Adducts of Carbon Dioxide to Magnesium, $(CO_2)MgX^-$ (X = OH, Cl, Br). *Angew. Chem., Int. Ed.* **2012**, *51*, 6938−6941.
(28) Miller, G. B. S.; Esser, T. K.; Knorke, H.; Gewinner, S.; Schöllkopf, W.; Heine, N.; Asmis, K. R.; Uggerud, E. Spectroscopic Identification of a Bidentate Binding Motif in the Anionic Magnesium-CO_2 Complex ($[ClMgCO_2]^-$). *Angew. Chem., Int. Ed.* **2014**, *53*, 14407−14410.
(29) Miller, G. B. S.; Uggerud, E. Dissociation of Mg(II) and Zn(II) Complexes of Simple 2-oxocarboxylates - Relationship to CO_2 Fixation, and the Grignard and Barbier Reactions. *Org. Biomol. Chem.* **2017**, *15*, 6813−6825.
(30) Miller, G. B. S.; Uggerud, E. C-C Bond Formation of Mg- and Zn-Activated Carbon Dioxide. *Chem. - Eur. J.* **2018**, *24*, 4710−4717.
(31) Knurr, B. J.; Weber, J. M. Solvent-Driven Reductive Activation of Carbon Dioxide by Gold Anions. *J. Am. Chem. Soc.* **2012**, *134*, 18804−18808.
(32) Menges, F. S.; Craig, S. M.; Tötsch, N.; Bloomfield, A.; Ghosh, S.; Krüger, H.-J.; Johnson, M. A. Capture of CO_2 by a Cationic Nickel(I) Complex in the Gas Phase and Characterization of the Bound, Activated CO_2 Molecule by Cryogenic Ion Vibrational Predissociation Spectroscopy. *Angew. Chem., Int. Ed.* **2016**, *55*, 1282−1285.
(33) Craig, S. M.; Johnson, C. J.; Ranasinghe, D. S.; Perera, A.; Bartlett, R. J.; Berman, M. R.; Johnson, M. A. Vibrational

DOI: 10.1021/acs.jpca.8b10530
J. Phys. Chem. A 2019, 123, 73−81

Characterization of Radical Ion Adducts between Imidazole and CO_2. *J. Phys. Chem. A* **2018**, *122*, 3805−3810.
(34) Plane, J. M. C.; Whalley, C. L. A New Model for Magnesium Chemistry in the Upper Atmosphere. *J. Phys. Chem. A* **2012**, *116*, 6240−6252.
(35) Whalley, C. L.; Martín, J. C. G.; Wright, T. G.; Plane, J. M. C. A Kinetic Study of Mg^+ and Mg-Containing Ions Reacting with O_3, O_2, N_2, CO_2, N_2O and H_2O: Implications for Magnesium Ion Chemistry in the Upper Atmosphere. *Phys. Chem. Chem. Phys.* **2011**, *13*, 6352−6364.
(36) Andersen, A.; Muntean, F.; Walter, D.; Rue, C.; Armentrout, P. B. Collision-Induced Dissociation and Theoretical Studies of Mg^+ Complexes with CO, CO_2, NH_3, CH_4, CH_3OH, and C_6H_6. *J. Phys. Chem. A* **2000**, *104*, 692−705.
(37) Dalleska, N. F.; Tjelta, B. L.; Armentrout, P. B. Sequential Bond Energies of Water to Na^+ (3s0), Mg^+ (3s1), and Al^+ (3s2). *J. Phys. Chem.* **1994**, *98*, 4191−4195.
(38) Rodriguez-Cruz, S. E.; Jockusch, R. A.; Williams, E. R. Hydration Energies and Structures of Alkaline Earth Metal Ions, $M^{2+}(H_2O)_n$, n = 5−7, M = Mg, Ca, Sr, and Ba. *J. Am. Chem. Soc.* **1999**, *121*, 8898−8906.
(39) Berg, C.; Beyer, M.; Achatz, U.; Joos, S.; Niedner-Schatteburg, G.; Bondybey, V. E. Stability and Reactivity of Hydrated Magnesium Cations. *Chem. Phys.* **1998**, *239*, 379−392.
(40) Berg, C.; Achatz, U.; Beyer, M.; Joos, S.; Albert, G.; Schindler, T.; Niedner-Schatteburg, G.; Bondybey, V. E. Chemistry and Charge Transfer Phenomena in Water Cluster Cations. *Int. J. Mass Spectrom. Ion Processes* **1997**, *167-168*, 723−734.
(41) Bauschlicher, C. W.; Sodupe, M.; Partridge, H. A Theoretical-Study of the Positive and Dipositive Ions of M(NH_3)N and M(H_2O)N for M = Mg, Ca, or Sr. *J. Chem. Phys.* **1992**, *96*, 4453−4463.
(42) Sanekata, M.; Misaizu, F.; Fuke, K.; Iwata, S.; Hashimoto, K. Reactions of Singly Charged Alkaline-Earth Metal Ions with Water Clusters: Characteristic Size Distribution of Product Ions. *J. Am. Chem. Soc.* **1995**, *117*, 747−754.
(43) Asada, T.; Iwata, S. Hybrid Procedure of ab Initio Molecular Orbital Calculation and Monte Carlo Simulation for Studying Intracluster Reactions: Applications to $Mg^+(H_2O)_n$ (n = 1−4). *Chem. Phys. Lett.* **1996**, *260*, 1−6.
(44) Watanabe, H.; Iwata, S.; Hashimoto, K.; Misaizu, F.; Fuke, K. Molecular-Orbital Studies of the Structures and Reactions of Singly Charged Magnesium-Ion with Water Clusters, $Mg^+(H_2O)_n$. *J. Am. Chem. Soc.* **1995**, *117*, 755−763.
(45) Reinhard, B. M.; Niedner-Schatteburg, G. Co-Existence of Hydrated Electron and Metal Di-Cation in $[Mg(H_2O)_n]^+$. *Phys. Chem. Chem. Phys.* **2002**, *4*, 1471−1477.
(46) Reinhard, B. M.; Niedner-Schatteburg, G. Ionization Energies and Spatial Volumes of the Singly Occupied Molecular Orbital in Hydrated Magnesium Clusters $[Mg,nH_2O]^+$. *J. Chem. Phys.* **2003**, *118*, 3571−3582.
(47) Misaizu, F.; Sanekata, M.; Tsukamoto, K.; Fuke, K.; Iwata, S. Photodissociation of Size-Selected Aquamagnesium $Mg^+(H_2O)_n$ Ions for n = 1 and 2. *J. Phys. Chem.* **1992**, *96*, 8259−8264.
(48) Misaizu, F.; Sanekata, M.; Fuke, K.; Iwata, S. Photodissociation Study on $Mg^+(H_2O)_n$, n = 1−5: Electronic Structure and Photo-induced Intracluster Reaction. *J. Chem. Phys.* **1994**, *100*, 1161−1170.
(49) Harms, A. C.; Khanna, S. N.; Chen, A. B.; Castleman, A. W. Dehydrogenation Reactions in $Mg^+(H_2O)_n$ Clusters. *J. Chem. Phys.* **1994**, *100*, 3540−3544.
(50) Willey, K. F.; Yeh, C. S.; Robbins, D. L.; Pilgrim, J. S.; Duncan, M. A. Photodissociation Spectroscopy of Mg^+−H_2O and Mg^+−D_2O. *J. Chem. Phys.* **1992**, *97*, 8886−8895.
(51) Ončák, M.; Taxer, T.; Barwa, E.; van der Linde, C.; Beyer, M. K. Photochemistry and Spectroscopy of Small Hydrated Magnesium Clusters $Mg^+(H_2O)_n$, n = 1−5. *J. Chem. Phys.* **2018**, *149*, 044309.
(52) Lam, T.-W.; van der Linde, C.; Akhgarnusch, A.; Hao, Q.; Beyer, M. K.; Siu, C.-K. Reduction of Acetonitrile by Hydrated Magnesium Cations $Mg^+(H_2O)_n$ ($n \approx$ 20−60) in the Gas Phase. *ChemPlusChem* **2013**, *78*, 1040−1048.
(53) Lam, T.-W.; Zhang, H.; Siu, C.-K. Reductions of Oxygen, Carbon Dioxide, and Acetonitrile by the Magnesium(II)/Magnesium-(I) Couple in Aqueous Media: Theoretical Insights from a Nano-Sized Water Droplet. *J. Phys. Chem. A* **2015**, *119*, 2780−2792.
(54) van der Linde, C.; Akhgarnusch, A.; Siu, C.-K.; Beyer, M. K. Hydrated Magnesium Cations $Mg^+(H_2O)_n$, $n \approx$ 20−60, Exhibit Chemistry of the Hydrated Electron in Reactions with O_2 and CO_2. *J. Phys. Chem. A* **2011**, *115*, 10174−10180.
(55) Gregoire, G.; Brinkmann, N. R.; van Heijnsbergen, D.; Schaefer, H. F.; Duncan, M. A. Infrared Photodissociation Spectroscopy of $Mg^+(CO_2)_n$ and $Mg^+(CO_2)_nAr$ Clusters. *J. Phys. Chem. A* **2003**, *107*, 218−227.
(56) Walker, N. R.; Walters, R. S.; Tsai, M.-K.; Jordan, K. D.; Duncan, M. A. Infrared Photodissociation Spectroscopy of $Mg^+(H_2O)Ar_n$. *J. Phys. Chem. A* **2005**, *109*, 7057−7067.
(57) Willey, K. F.; Yeh, C. S.; Robbins, D. L.; Duncan, M. A. Photodissociation Spectroscopy of Mg^+CO_2. *Chem. Phys. Lett.* **1992**, *192*, 179−184.
(58) van der Linde, C.; Höckendorf, R. F.; Balaj, O. P.; Beyer, M. K. Reactions of Hydrated Singly Charged First-Row Transition-Metal Ions $M^+(H_2O)_n$ (M = V, Cr, Mn, Fe, Co, Ni, Cu, and Zn) toward Nitric Oxide in the Gas Phase. *Chem. - Eur. J.* **2013**, *19*, 3741−3750.
(59) van der Linde, C.; Hemmann, S.; Höckendorf, R. F.; Balaj, O. P.; Beyer, M. K. Reactivity of Hydrated Monovalent First Row Transition Metal Ions $M^+(H_2O)_n$, M = V, Cr, Mn, Fe, Co, Ni, Cu, Zn, toward Molecular Oxygen, Nitrous Oxide, and Carbon Dioxide. *J. Phys. Chem. A* **2013**, *117*, 1011−1020.
(60) Siu, C. K.; Liu, Z. F. Ab Initio Studies on the Mechanism of the Size-Dependent Hydrogen-Loss Reaction in $Mg^+(H_2O)_n$. *Chem. - Eur. J.* **2002**, *8*, 3177−3186.
(61) Akhgarnusch, A.; Höckendorf, R. F.; Beyer, M. K. Thermochemistry of the Reaction of SF_6 with Gas-Phase Hydrated Electrons: A Benchmark for Nanocalorimetry. *J. Phys. Chem. A* **2015**, *119*, 9978−9985.
(62) Berg, C.; Schindler, T.; Niedner-Schatteburg, G.; Bondybey, V. E. Reactions of Simple Hydrocarbons with Nb_n^+: Chemisorption and Physisorption on Ionized Niobium Clusters. *J. Chem. Phys.* **1995**, *102*, 4870−4884.
(63) Caravatti, P.; Allemann, M. The Infinity Cell: A New Trapped-Ion Cell with Radiofrequency Covered Trapping Electrodes for Fourier Transform Ion Cyclotron Resonance Mass Spectrometry. *Org. Mass Spectrom.* **1991**, *26*, 514−518.
(64) Bondybey, V. E.; English, J. H. Laser Induced Fluorescence of Metal Clusters Produced by Laser Vaporization: Gas Phase Spectrum of Pb_2. *J. Chem. Phys.* **1981**, *74*, 6978−6979.
(65) Dietz, T. G.; Duncan, M. A.; Powers, D. E.; Smalley, R. E. Laser Production of Supersonic Metal Cluster Beams. *J. Chem. Phys.* **1981**, *74*, 6511−6512.
(66) Beyer, M.; Berg, C.; Görlitzer, H. W.; Schindler, T.; Achatz, U.; Albert, G.; Niedner-Schatteburg, G.; Bondybey, V. E. Fragmentation and Intracluster Reactions of Hydrated Aluminum Cations $Al^+(H_2O)_n$, n = 3−50. *J. Am. Chem. Soc.* **1996**, *118*, 7386−7389.
(67) Marshall, A. G.; Hendrickson, C. L.; Jackson, G. S. Fourier Transform Ion Cyclotron Resonance Mass Spectrometry: A Primer. *Mass Spectrom. Rev.* **1998**, *17*, 1−35.
(68) Thölmann, D.; Tonner, D. S.; McMahon, T. B. Spontaneous Unimolecular Dissociation of Small Cluster Ions, $(H_3O^+)L_n$ and $Cl^-(H_2O)_n$ (n = 2−4), under Fourier Transform Ion Cyclotron Resonance Conditions. *J. Phys. Chem.* **1994**, *98*, 2002−2004.
(69) Dunbar, R. C. Kinetics of Thermal Unimolecular Dissociation by Ambient Infrared Radiation. *J. Phys. Chem.* **1994**, *98*, 8705−8712.
(70) Schindler, T.; Berg, C.; Niedner-Schatteburg, G.; Bondybey, V. E. Protonated Water Clusters and Their Black Body Radiation Induced Fragmentation. *Chem. Phys. Lett.* **1996**, *250*, 301−308.
(71) Schnier, P. D.; Price, W. D.; Jockusch, R. A.; Williams, E. R. Blackbody Infrared Radiative Dissociation of Bradykinin and its Analogues: Energetics, Dynamics, and Evidence for Salt-Bridge Structures in the Gas Phase. *J. Am. Chem. Soc.* **1996**, *118*, 7178−7189.

DOI: 10.1021/acs.jpca.8b10530
J. Phys. Chem. A 2019, 123, 73−81

(72) Dunbar, R. C.; McMahon, T. B. Activation of Unimolecular Reactions by Ambient Blackbody Radiation. *Science* **1998**, *279*, 194−197.
(73) Lee, S. W.; Freivogel, P.; Schindler, T.; Beauchamp, J. L. Freeze-Dried Biomolecules: FT-ICR Studies of the Specific Solvation of Functional Groups and Clathrate Formation Observed by the Slow Evaporation of Water from Hydrated Peptides and Model Compounds in the Gas Phase. *J. Am. Chem. Soc.* **1998**, *120*, 11758−11765.
(74) Fox, B. S.; Beyer, M. K.; Bondybey, V. E. Black Body Fragmentation of Cationic Ammonia Clusters. *J. Phys. Chem. A* **2001**, *105*, 6386−6392.
(75) Dunbar, R. C. BIRD (Blackbody Infrared Radiative Dissociation): Evolution, Principles, and Applications. *Mass Spectrom. Rev.* **2004**, *23*, 127−158.
(76) Daneshfar, R.; Klassen, J. S. Arrhenius Activation Parameters for the Loss of Neutral Nucleobases from Deprotonated Oligonucleotide Anions in the Gas Phase. *J. Am. Soc. Mass Spectrom.* **2004**, *15*, 55−64.
(77) Savchenko, E. V.; Ogurtsov, A. N.; Grigorashchenko, O. N.; Beyer, M.; Lorenz, M.; Lammers, A.; Bondybey, V. E. Radiation-Induced Formation of Stable Charge Centers in Rare-Gas Solids. *Nucl. Instrum. Methods Phys. Res., Sect. B* **2000**, *166-167*, 47−50.
(78) Donald, W. A.; Leib, R. D.; O'Brien, J. T.; Williams, E. R. Directly Relating Gas-Phase Cluster Measurements to Solution-Phase Hydrolysis, the Absolute Standard Hydrogen Electrode Potential, and the Absolute Proton Solvation Energy. *Chem. - Eur. J.* **2009**, *15*, 5926−5934.
(79) Schindler, T.; Berg, C.; Niedner-Schatteburg, G.; Bondybey, V. E. Gas-Phase Reactivity of Sulfur Cluster Cations and Anions by FT-ICR Investigations. *Ber. Bunsen-Ges. Phys. Chem.* **1992**, *96*, 1114−1120.
(80) Schröder, D.; Schwarz, H.; Clemmer, D. E.; Chen, Y. M.; Armentrout, P. B.; Baranov, V. I.; Bohme, D. K. Activation of Hydrogen and Methane by Thermalized FeO^+ in the Gas Phase as Studied by Multiple Mass Spectrometric Techniques. *Int. J. Mass Spectrom. Ion Processes* **1997**, *161*, 175−191.
(81) Schmidt, M.; von Issendorff, B. Gas-Phase Calorimetry of Protonated Water Clusters. *J. Chem. Phys.* **2012**, *136*, 164307.
(82) Hock, C.; Schmidt, M.; Kuhnen, R.; Bartels, C.; Ma, L.; Haberland, H.; von Issendorff, B. Calorimetric Observation of the Melting of Free Water Nanoparticles at Cryogenic Temperatures. *Phys. Rev. Lett.* **2009**, *103*, 73401.
(83) Su, T.; Bowers, M. T. Ion-Polar Molecule Collisions - Proton-Transfer Reactions of H_3^+ and CH_5^+ to Geometric Isomers of Difluoroethylene, Dichloroethylene, and Difluorobenzene. *J. Am. Chem. Soc.* **1973**, *95*, 1370−1373.
(84) Su, T.; Bowers, M. T. Theory of Ion-Polar Molecule Collisions - Comparison with Experimental Charge-Transfer Reactions of Rare-Gas Ions to Geometric Isomers of Difluorobenzene and Dichloroethylene. *J. Chem. Phys.* **1973**, *58*, 3027−3037.
(85) Kummerlöwe, G.; Beyer, M. K. Rate Estimates for Collisions of Ionic Clusters with Neutral Reactant Molecules. *Int. J. Mass Spectrom.* **2005**, *244*, 84−90.
(86) Donald, W. A.; Leib, R. D.; Demireva, M.; Negru, B.; Neumark, D. M.; Williams, E. R. Average Sequential Water Molecule Binding Enthalpies of $M(H_2O)_{19-124}^{2+}$ (M = Co, Fe, Mn, and Cu) Measured with Ultraviolet Photodissociation at 193 and 248 nm. *J. Phys. Chem. A* **2011**, *115*, 2−12.
(87) Zhao, Y.; Truhlar, D. G. The M06 Suite of Density Functionals for Main Group Thermochemistry, Thermochemical Kinetics, Noncovalent Interactions, Excited States, and Transition Elements: Two New Functionals and Systematic Testing of Four M06-Class Functionals and 12 Other Functionals. *Theor. Chem. Acc.* **2008**, *120*, 215−241.
(88) Plowright, R. J.; McDonnell, T. J.; Wright, T. G.; Plane, J. M. C. Theoretical Study of Mg^+-X and $[X\text{-}Mg\text{-}Y]^+$ Complexes Important in the Chemistry of Ionospheric Magnesium (X, Y = H_2O, CO_2, N_2, O_2, and O). *J. Phys. Chem. A* **2009**, *113*, 9354−9364.
(89) Montgomery, J. A.; Frisch, M. J.; Ochterski, J. W.; Petersson, G. A. A Complete Basis Set Model Chemistry. VI. Use of Density Functional Geometries and Frequencies. *J. Chem. Phys.* **1999**, *110*, 2822−2827.
(90) Breneman, C. M.; Wiberg, K. B. Determining Atom-Centered Monopoles from Molecular Electrostatic Potentials. The Need for High Sampling Density in Formamide Conformational Analysis. *J. Comput. Chem.* **1990**, *11*, 361−373.
(91) Frisch, M. J.; Trucks, G. W.; Schlegel, H. B.; Scuseria, G. E.; Robb, M. A.; Cheeseman, J. R.; Scalmani, G.; Barone, V.; Mennucci, B.; Petersson, G. A., et al. *Gaussian 09, Revision D.01*; Gaussian Inc.: Wallingford, CT, 2013.
(92) Hollas, D.; Svoboda, O.; Ončák, M.; Slavíček, P. ABIN, Source code available at https://github.com/PHOTOX/ABIN.
(93) Gilbert, R. G.; Smith, S. C. *Theory of Unimolecular and Recombination Reactions; Physical Chemistry Texts*; Blackwell Scientific Publications: Oxford, U.K., 1990.
(94) Whalley, C. L.; Plane, J. M. C. Meteoric Ion Layers in the Martian Atmosphere. *Faraday Discuss.* **2010**, *147*, 349.

DOI: 10.1021/acs.jpca.8b10530
J. Phys. Chem. A 2019, 123, 73−81